Available online at www.sciencedirect.com
ScienceDirect
International Journal of Heat and Mass Transfer 50 (2007) 1516–1527
International Journal of HEAT and MASS TRANSFER
www.elsevier.com/locate/ijhmt

Infrared radiative properties of polymer coatings containing hollow microspheres

Leonid A. Dombrovsky [a,*], Jaona H. Randrianalisoa [b], Dominique Baillis [b]

[a] Institute for High Temperatures of the Russian Academy of Sciences, Krasnokazarmennaya 17A, NCHMT, Moscow 111116, Russia
[b] Centre de Thermique de Lyon, Institut National des Sciences Appliqués, Lyon, 69621 Villeurbanne Cedex, France

Received 2 May 2006; received in revised form 23 August 2006
Available online 7 November 2006

Abstract

Infrared radiative properties of a polymer containing hollow glass microspheres are studied by means of the measurements of directional-hemispherical reflectance and transmittance in the wavelength range from 2.6 to 18 μm. The measurements are performed for several samples containing different series of microspheres of volume fraction from about 6% to 66%. Relatively strong peak of reflectance at the wavelength 4.5 μm was observed. This peak is explained in terms of theoretical model based on Mie theory calculations for single microspheres and modified two-flux approximation proposed recently by the authors. The reflectance of the composite material in the important range from 8.5 to 13.5 μm is determined mainly by rough surface layer of microspheres and it does not described by the model for semi-transparent media. The conditions of a considerable decrease in radiative heat losses from the buildings due to paint coatings containing hollow glass microspheres are discussed.

Keywords: Radiation; Infrared; Absorption; Scattering; Coating; Microspheres

1. Introduction

In recent years, composite materials containing hollow glass or ceramic microspheres have attracted considerable attention. Such materials exhibit unusual mechanical properties and high heat-insulation characteristics, which are largely defined by special features of absorption and scattering of thermal radiation by thin-walled hollow particles [1,2]. Therefore, a number of developments associated with the production of glass microspheres are oriented toward development of heat-insulating coatings. Such coatings have already found application for the purpose of reducing the heat loss from the walls of buildings owing to a decrease in thermal radiation at night. Present-day technical potentialities enable one to manufacture glass microspheres of different geometric parameters. The choice of disperse composition of microspheres for use in building paints and other polymer coatings remains a problem which requires theoretical and experimental investigation.

Theoretical prediction of wide-range spectral radiative properties of the coatings containing polydisperse hollow microspheres based on traditional radiation transfer model in combination with the Mie theory for single particles (as was suggested in paper [2]) may be not adequate at high concentration of microspheres because of specific scattering effects in the volume and at the coating interface. It is known that the so-called dependent scattering effects can be observed in densely-packed disperse systems [3–7].

We are presenting now probably the first experimental study of the main radiative properties of polymer films with microspheres in spectral range from 2.6 to 18 μm. The measurements of directional-hemispherical reflectance and transmittance of coatings at various concentrations of hollow glass microspheres were performed by use of FTIR spectrometer. The new experimental data are compared

* Corresponding author.
E-mail address: dombr@online.ru (L.A. Dombrovsky).

0017-9310/$ - see front matter © 2006 Elsevier Ltd. All rights reserved.
doi:10.1016/j.ijheatmasstransfer.2006.08.034

Nomenclature

a	particle radius
A, B, C, D, D_1, E	coefficients in analytical solutions (4), (8) and (11)
D	thickness of the sample
f_v	volume fraction of microspheres
F	particle size distribution
h	height of roughness
k_1, k_2	coefficients in Eq. (9)
n	index of refraction
N	number of points in the roughness measurements
P	parameter defined by Eq. (18)
Q_a	efficiency factor of absorption
Q_s^{tr}	transport efficiency factor of scattering
r_1	coefficient in the reflectance approximation
R	reflectance
R_0	specular reflectance
R_1	normal reflectance from smooth surface
s, c	designations of hyperbolic functions (13)
Y	coordinate along the surface
T	transmittance
x	diffraction parameter

Greek symbols

α	absorption coefficient
α_1	absorption parameter
β	eigenvalue of the problem
γ, $\bar{\gamma}$	coefficients in boundary conditions
δ	wall thickness of microsphere
κ	index of absorption
λ	radiation wavelength
$\bar{\mu}$	asymmetry factor of scattering
μ_c	cosine of the critical angle defined by Eq. (13)
ε	emissivity
ρ	density of material
σ	scattering coefficient
τ	optical thickness
φ	coefficient in Eqs. (9) and (10)
ω	albedo

Subscripts and superscripts

a	absorption
d	diffuse
d-h	directional-hemispherical
g	glass
h	hemispherical
m	microspheres
s	scattering
t	total
tr	transport
λ	spectral
0	polymer matrix, referenced value

with theoretical predictions based on the hypothesis of negligible role of dependent scattering effects.

The hemispherical emissivity of optically thick coatings containing hollow glass microspheres is analyzed to find the conditions of considerable decrease in radiative heat losses from the building walls during clear sky nights.

2. Samples of composite material and experimental procedure

Two series of hollow glass microspheres produced by 3M Company were used to prepare the samples of composite material. The normalized size distributions $F(a)$ for microspheres K20 and S38 are shown in Fig. 1. These distributions were obtained from volume distributions given by 3M Company. To estimate an average wall thickness of microspheres one can use the following equations assuming the definite relation between the wall thickness δ and particle radius a:

$$\rho_m = 3\rho_g \frac{\bar{\delta}}{a_{32}}, \quad \bar{\delta} = \frac{1}{a_{20}} \int_0^\infty \delta(a) a^2 F(a)\, da \tag{1}$$

where ρ_g is the density of glass, ρ_m is the apparent density of polydisperse microspheres, and the parameters a_{ij} are defined as follows:

$$a_{ij} = \int_0^\infty a^i F(a)\, da \Big/ \int_0^\infty a^j F(a)\, da \tag{2}$$

It is known that $a_{32} = 50$ μm, $\rho_m = 0.202$ g/cm^3 for K20 and $a_{32} = 40.7$ μm, $\rho_m = 0.387$ g/cm^3 for S38 microspheres. Substituting these values and $\rho_g = 2.54$ g/cm^3 for soda lime borosilicate glass in Eq. (1), one can find the average wall thickness $\bar{\delta}$

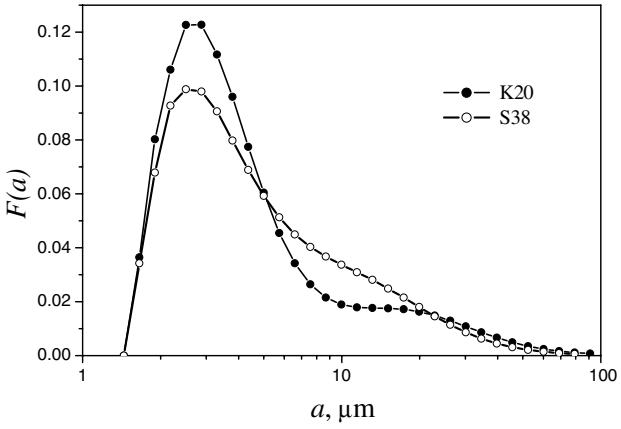

Fig. 1. Normalized size distributions of glass microspheres.

$$\bar{\delta} = a_{32}\frac{\rho_m}{3\rho_g} = \begin{cases} 1.3\ \mu m & \text{for K20} \\ 2.1\ \mu m & \text{for S38} \end{cases} \quad (3)$$

We have no data for the dependence of $\delta(a)$. For this reason, the further analysis will be based on the results for the following two assumptions: $\delta = \bar{\delta} = \text{const}$ or $\delta = \bar{\delta}a/a_{32}$.

The samples of composite material were made by mixing of glass microspheres in polymer ACRONAL 290D, which is made from emulsion of styrene-acrylique from BASF Corporation. The mixture was spread out over a plane surface and it was then dried. The resulting parameters of thin square samples of area 16 cm^2 are given in Table 1. When the polymer layer dries out, the distance between the microspheres decreases differently in different directions. This results in the anisotropy of the volume concentration of microspheres and in the respective anisotropy of the radiative characteristics of the medium [2]. The estimates showed that this effect is not significant and we assume the composite material to be homogeneous and isotropic.

Because of specific manufacturing process, the one side of each sample was relatively smooth while the other side appears to be rougher. Two typical microphotos of rough side view of the samples are presented in Fig. 2. The majority of particles are ideal spheres but some of large particles are damaged (at least, near the sample surface). One can see also several irregular small fragments of the glass microspheres. The roughness profiles of the sample surfaces $h(s)$ were measured by using wide-field confocal microscope MICROSME-2 with the interval $\Delta y = 5\ \mu m$ at distance $y_0 = 10\ mm$. The average height of the roughness $h(y)$ was determined as follows:

$$\bar{h} = \frac{1}{N}\sqrt{\sum_{i=1}^{N}[h(y_i) - h_0]^2}, \quad h_0 = \frac{1}{N}\sum_{i=1}^{N} h(y_i) \quad (4)$$

The value of $\bar{h}$ for pure polymer film appears to be equal to 3.5 μm for the rough side and 0.7 μm for the smooth side. The other values obtained for the samples containing glass microspheres are given in Table 2. One can see that the

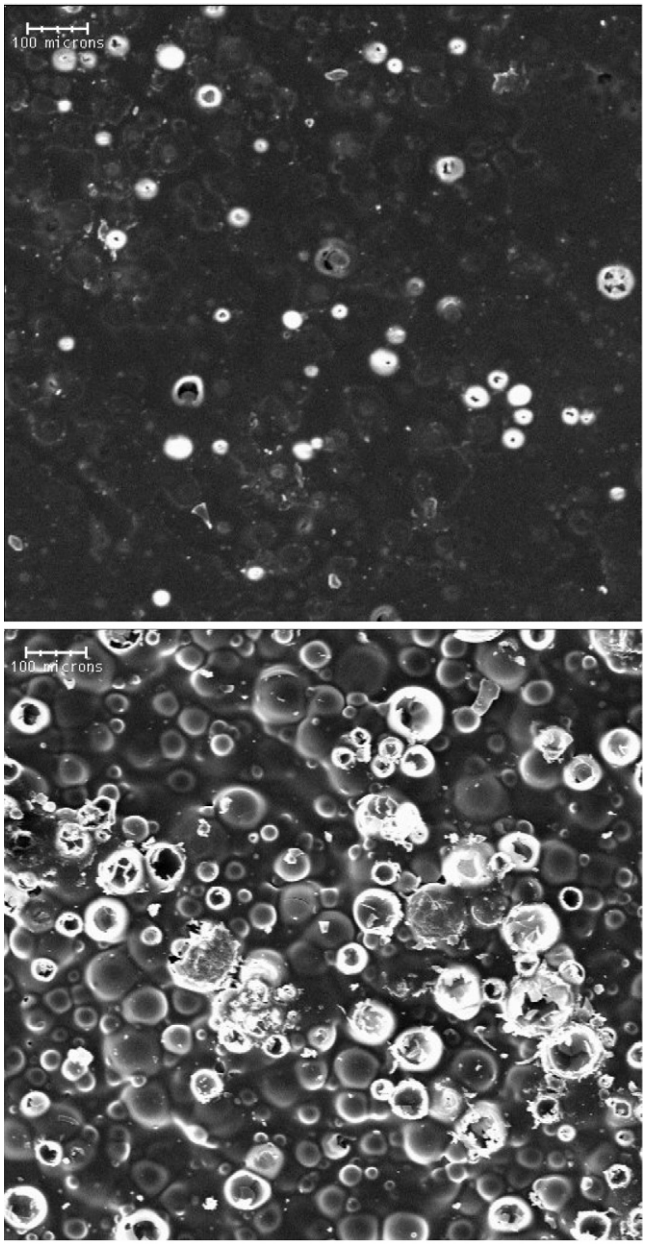

Fig. 2. The fragments of the rough surface of the polymer samples containing microspheres of series K20: the upper image – sample 1, the lower – sample 5 (see Table 1).

Table 1
The main parameters of the samples

Type of microspheres	Sample number	Thickness, d (μm)	Thickness deviation, Δd (μm)	Volume fraction of microspheres, f_v (%)	Volume fraction uncertainty, Δf_v (%)
K20	1	141.9	3.2	6.6	3.4
	2	138.9	8.0	23.3	7.4
	3	140.2	5.6	37.4	4.4
	4	156.6	4.8	50.1	2.9
	5	174.9	3.5	65.4	1.5
S38	1	142.6	5.7	9.6	6.0
	2	144.7	2.0	23.4	1.8
	3	149.4	4.9	38.2	3.9
	4	152.2	5.9	52.8	4.1
	5	165.6	4.4	66.4	2.4

Table 2
The average height of sample roughness

Type of microspheres	Sample number	$\bar{h}$ (μm)	
		Smooth surface	Rough surface
K20	1	–	5.0
	2	–	7.9
	3	–	9.2
	4	–	14.8
	5	–	18.9
S38	1	0.7	3.5
	2	0.9	5.4
	3	1.1	6.4
	4	1.5	10.2
	5	2.0	14.0

height of roughness increases with the volume fraction and with the average size of microspheres. To analyze the effect of the surface roughness on reflectance and transmittance, all the measurements were performed for two orientations of the samples with respect to the collimated incident radiation.

The samples of polymer film containing glass microspheres are illuminated by a collimated beam incident at the angle 10° to the normal direction. The experimental set-up consists of two main parts: a BIO-RAD FTS 60A FTIR spectrometer and a gold-coated integrating sphere CSTM RSA-DI-40D which collects hemispherically the radiation crossing or reflected by the sample onto a detector placed on the wall of the sphere. Not only the total reflectance and transmittance were measured but also their diffuse components, which do not include the specularly reflected radiation and the radiation transmitted in the direction of the incident collimated beam. In contrast to similar measurements for fused quartz containing gas bubbles [8] the spectra of directional-hemispherical reflectance and transmittance are not very noisy. The standard absolute deviation is less than 5% for both transmittance and reflectance in the entire spectral range.

3. Optical properties of substances

Spectral optical constants of the polymer were obtained from the measurements of reflectance and transmittance for pure polymer film of thickness 20 μm. The well-known relations were used for calculating the index of refraction n_0 and the index of absorption κ_0 of the polymer [9]. The data obtained from the measurements at various angles of incidence were averaged to find more accurate results shown in Fig. 3.

The glass microspheres are made from soda lime borosilicate glass (75% SiO_2, 4% Na_2O, 15% CaO, and 6% B_2O_3). To the best of our knowledge, there is no data for optical constants of this glass in the literature. The wide-range infrared optical constants of soda lime silica glasses were investigated in paper [10]. The tabulated results for a typical clear window glass (73% SiO_2, 15% Na_2O, 10% CaO, and 2% Al_2O_3) are plotted in Fig. 3. We performed also the measurements for low expansion borosilicate glass supplied by Verre Labo Mula Company: 81% SiO_2, 4% Na_2O, 13% B_2O_3 and 2% Al_2O_3. The optical constants of this glass in the wavelength range $3 < \lambda < 5$ μm were determined from the reflectance and transmittance measurements for the sample of thickness 0.7 mm by use of the same experimental technique as that used for polymer. The optical constants in the range $7 < \lambda < 18$ μm were obtained by use of the least squares optimization technique and experimental data for specular reflectance in the angular range from 13° to 80°. The wide-range optical constants of borosilicate glass are also presented in Fig. 4. The spectral behavior of optical constants for two types of glasses is similar but one can see considerable quantitative differences both in the range of semi-transparency and in the long-wave region. The effect of optical constants uncertainty on radiative properties of microspheres and composite material will be analyzed below.

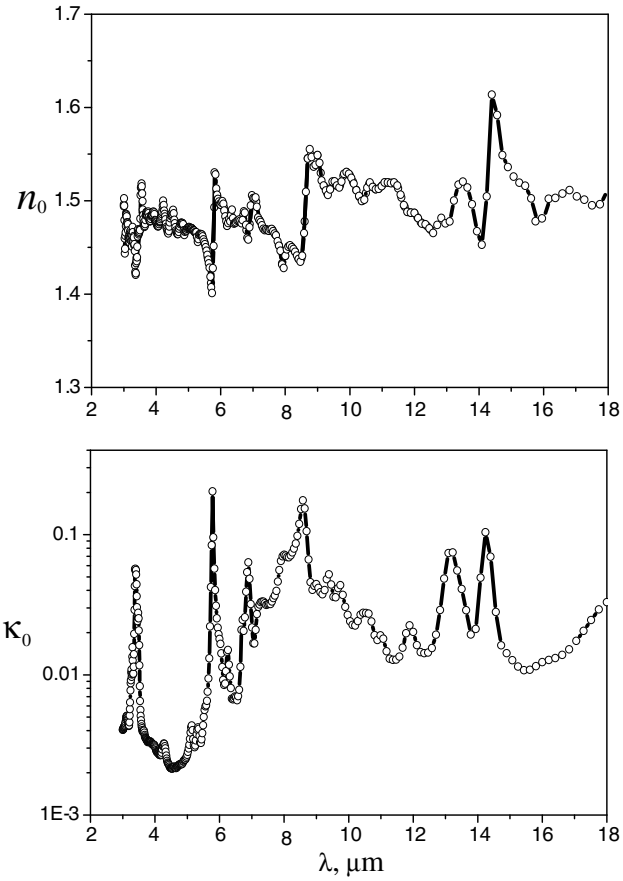

Fig. 3. Optical constants of polymer.

4. Experimental results for transmittance and reflectance

Consider first the total and diffuse directional-hemispherical characteristics for the case of orientation of the samples toward the incident radiation by a relatively

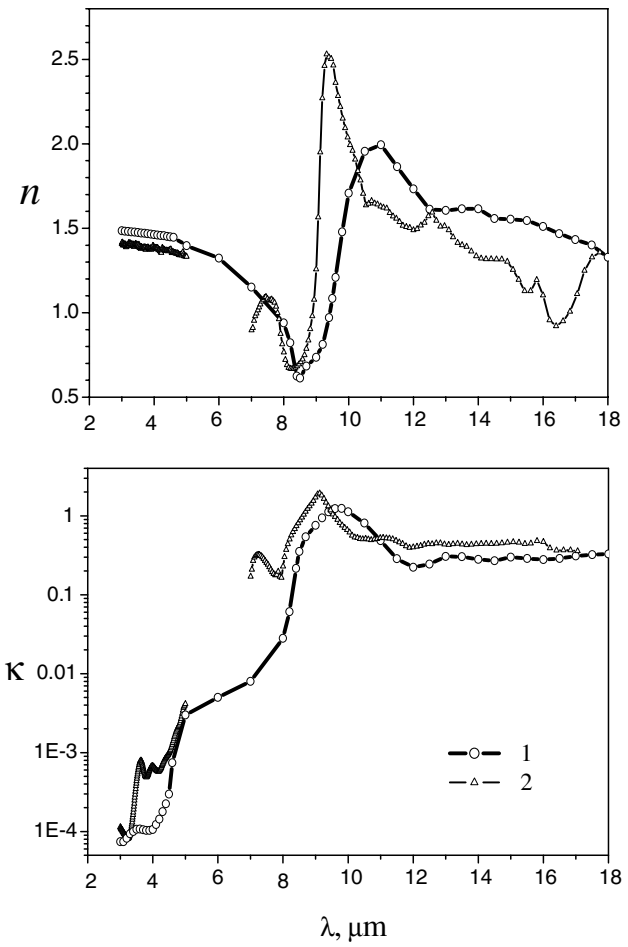

Fig. 4. Optical constants of glasses: (1) soda lime silica glass [10], (2) borosilicate glass (present paper).

smooth surface (the case of smooth front surface). The data for samples of number 1, 3, and 5 are presented in Fig. 5 (intermediate curves for samples 2 and 4 are not shown in the graph). One can see significant increase in directional-hemispherical reflectance due to scattering of radiation by microspheres. This increase in reflectance is approximately proportional to the volume fraction of microspheres:

$$R^{t}_{d\text{-}h} = R_0 + R^{d}_{d\text{-}h}, \quad R^{d}_{d\text{-}h} = f_v r_1 \tag{5}$$

where R_0 is the specular reflectance of the polymer sample without microspheres. Such behavior of diffuse reflectance with particle concentration is typical for independently scattering particles in a weakly absorbing medium. It is interesting that the value of r_1 is not sensitive to the type of microspheres. The peak of $r_1(\lambda)$ at the wavelength 4.5 μm is a result of intense scattering of the radiation by hollow glass microspheres.

The microspheres decrease the directional-hemispherical transmittance of the polymer samples. This effect depends on the type of microspheres (at least for $f_v \geqslant 30\%$) and cannot be described by linear function of volume fraction f_v as it was done for the reflectance. It is important that specular component of transmitted radiation is not small: about a half of the transmitted radiation is concentrated near the forward direction.

The experimental data for the case of rougher front surface of the samples are presented in Fig. 6. In this case, there is no specular reflection from the front surface. At the same time, the radiation propagating through the front surface is mainly concentrated near the forward direction and the reflection from smoother back (shadow) surface gives specular component in the total reflectance of the sample. The last effect is considerable only for small volume fraction of microspheres. Note that reflectance in the range $9 < \lambda < 13$ μm is sensitive to the type of microspheres. This effect was not observed when the samples are oriented to the incident radiation by their smoother surface.

It is interesting that the short-wave peak of total reflectance at $\lambda = 4.5$ μm is insensitive to both the sample orientation and the type of microspheres. The same statement is true for the corresponding peak of total transmittance. In contrast to the reflection, one can observe considerable specular transmission of the radiation in the case of rough front surface and smooth back surface of the sample. This result is clear if we remember that the rougher front surface does not prevent concentration of the propagated radiation near the forward direction. As for diffuse transmittance, it is practically the same for various orientations of the sample.

5. Theoretical modelling of directional-hemispherical characteristics of polymer layer containing hollow microspheres

In this paper, we consider a theoretical model based on modified two-flux approximation for the radiation transfer and the Mie theory for scattering of radiation by single hollow glass particles embedded in the polymer matrix. This approach can be used when dependent scattering effects are not significant. The latter assumption should be verified by comparison of theoretical predictions with experimental data.

The modified two-flux approach suggested in papers [8,11] for the normally incident collimated radiation is applied to the radiation transfer equation for the model transport scattering function. The use of transport approximation enables us to separate the real diffuse component of the radiation field in the case of collimated incident radiation. The subsequent approximation of the angular dependence of the diffuse radiation component includes the angle intervals which are determined by total internal reflection and depend on refractive index of the host medium. For the refracting medium, these angle intervals are not hemispheres as in the well-known ordinary two-flux method. The mathematical problem statement for a layer of homogeneous medium can be found in paper [11]. We

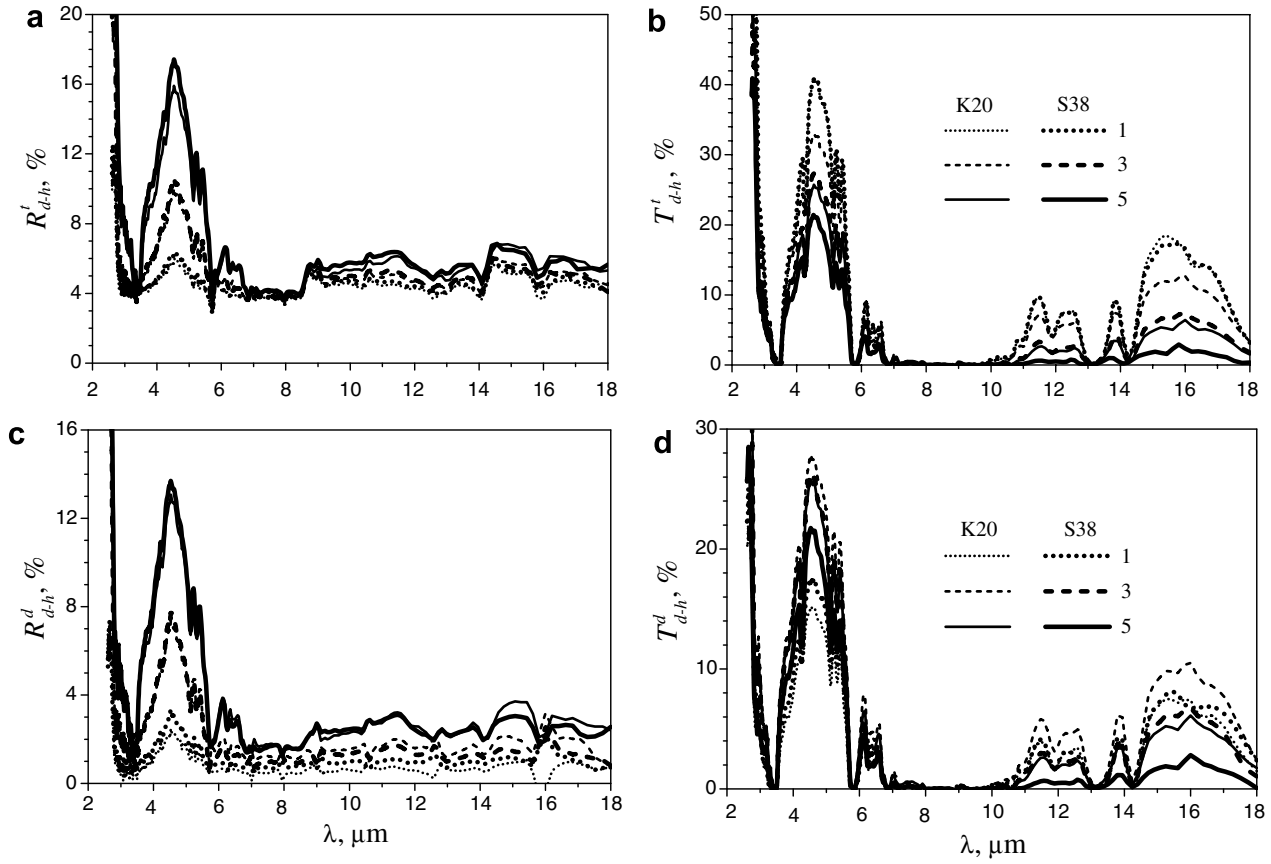

Fig. 5. Total (a and b) and diffuse (c and d) reflectance and transmittance of polymer samples containing glass microspheres: (1, 3 and 5) sample numbers. The samples are oriented to the incident radiation by their smooth surfaces.

use the derived analytical solution of the boundary-value problem to calculate the directional-hemispherical reflectance and transmittance of a homogeneous medium layer with perfectly smooth surfaces. In the case of nonscattering refracting medium, the reflectance and transmittance of the medium layer are expressed as follows [9]:

$$R_0 = \frac{R_1 + (1-R_1)^2 C}{1 - R_1 C}, \quad T_0 = \frac{(1-R_1)^2 E}{1 - R_1 C} \tag{6}$$

where

$$R_1 = \left(\frac{n_0 - 1}{n_0 + 1}\right)^2, \quad C = R_1 E^2, \quad E = \exp(-\tau_{\mathrm{tr}}) \tag{7}$$

In this case, the transport optical thickness of the layer $\tau_{\mathrm{tr}} = (\alpha + \sigma_{\mathrm{tr}})d$ is determined only by absorption coefficient of the medium α and the layer thickness d. In the general case of a scattering medium, one should take into account the transport scattering coefficient $\sigma_{\mathrm{tr}} = \sigma(1 - \bar{\mu})$, where σ is the usual scattering coefficient, $\bar{\mu}$ is the asymmetry factor of scattering. Eqs. (6) and (7) remain the same but they give only directional components of reflectance and transmittance. The expressions for directional-hemispherical characteristics $R_{\mathrm{d\text{-}h}}$ and $T_{\mathrm{d\text{-}h}}$ are given below. As was shown in paper [11] these expressions are different for parameter $\beta = 1$ and $\beta \neq 1$. In the first case, we have

$$R_{\mathrm{d\text{-}h}} = R_0 + D_1 B, \quad T_{\mathrm{d\text{-}h}} = T_0 + D_1[A + \tau_{\mathrm{tr}}(1 + R_1)E]$$

$$D_1 = \frac{\gamma}{2n_0^2} \frac{\omega_{\mathrm{tr}}}{1 - \omega_{\mathrm{tr}}} \frac{1 - R_1}{1 - R_1 C} \tag{8}$$

$$A = \frac{k_1(\varphi s + c)E + k_2}{(1 + \varphi^2)s + 2\varphi c}, \quad B = \frac{k_1 E + k_2(\varphi s + c)}{(1 + \varphi^2)s + 2\varphi c} \tag{9}$$

$$k_1 = (1 + R_1)\tau_{\mathrm{tr}} - (1 - R_1)(1 + \varphi\tau_{\mathrm{tr}}), \quad k_2 = 1 - C \tag{10}$$

In the second case, Eq. (9) is the same but Eqs. (8) and (10) should be replaced by the following ones:

$$R_{\mathrm{d\text{-}h}} = R_0 + D\left(1 + \frac{B}{\beta} + C\right), \quad T_{\mathrm{d\text{-}h}} = T_0 + D\left[\frac{A}{\beta} + (1 + R_1)E\right]$$

$$D = D_1 \frac{\beta^2}{\beta^2 - 1} \tag{11}$$

$$k_1 = (1 - 2\bar{\gamma}) - (1 + 2\bar{\gamma})R_1, \quad k_2 = (1 - 2\bar{\gamma})C - (1 + 2\bar{\gamma}) \tag{12}$$

The following designations are used in the equations presented above:

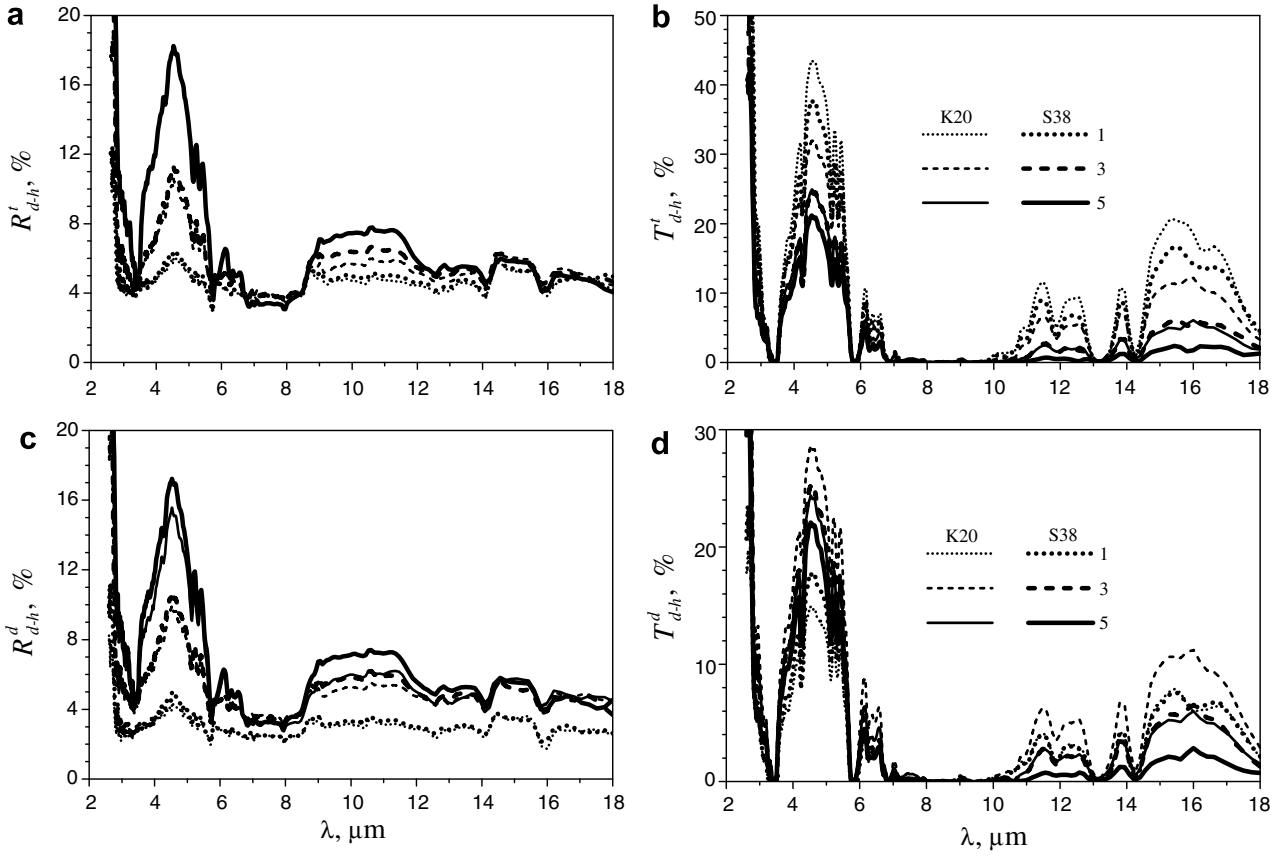

Fig. 6. Total (a and b) and diffuse (c and d) reflectance and transmittance of polymer samples containing microspheres: (1, 3 and 5) sample numbers. The samples are oriented to the incident radiation by their rough surfaces.

$$\varphi = 2\bar{\gamma}/\beta, \quad \bar{\gamma} = \gamma/(1+\mu_c), \quad s = \sinh(\beta\tau_{tr}),$$
$$c = \cosh(\beta\tau_{tr}), \quad \beta = \frac{2}{1+\mu_c}\sqrt{\frac{1-\omega_{tr}}{1-\omega_{tr}\mu_c}},$$
$$\omega_{tr} = \frac{\sigma_{tr}}{\alpha+\sigma_{tr}}, \quad \gamma = \frac{1-R_1}{1+R_1} = \frac{2n_0}{n_0^2+1}, \quad \mu_c = \sqrt{1-\frac{1}{n_0^2}} \tag{13}$$

Note that there is no need in expressions for $\beta = 1$ in practical calculations because the solution is continuous and same results can be obtained for close values of β.

It was shown in papers [8,11] that the modified two-flux approximation gives rather accurate results for the directional-hemispherical characteristics. For the values of reflectance and transmittance typical for semi-transparency ranges of the polymer film, the error of this approach is less than 3%.

Three spectral characteristics of an absorbing and anisotropically scattering medium are included as coefficients in the modified two-flux approximation: the index of refraction of the host medium n_0, the absorption coefficient of the composite material α and the transport scattering coefficient of polydisperse particles σ_{tr}. The absorption and transport scattering coefficients can be determined as follows [2,12,13]:

$$\alpha = \alpha_0 + 0.75\frac{f_v}{a_{30}}\int_0^\infty Q_a a^2 F(a)\,da,$$
$$\sigma_{tr} = 0.75\frac{f_v}{a_{30}}\int_0^\infty Q_s^{tr} a^2 F(a)\,da \tag{14}$$

where $\alpha_0 = 4\pi\kappa_0/\lambda$ is the absorption coefficient of the host medium (polymer matrix), Q_a, Q_s^{tr} are the efficiency factor of absorption and transport efficiency factor of scattering for single spherical particles. The efficiency factors Q_a, Q_s^{tr} can be calculated by the Mie theory generalized to the case of refracting and absorbing medium as described in paper [2]. In the monodisperse approximation, which is often used in engineering calculations [12], Eq. (14) is reduced to the following ones:

$$\alpha = \alpha_0 + 0.75\frac{f_v Q_a(a_{32})}{a_{32}}, \quad \sigma_{tr} = 0.75\frac{f_v Q_s^{tr}(a_{32})}{a_{32}} \tag{15}$$

Note that monodisperse approximation gives the exact results for polydisperse systems in the case of constant efficiency factors as well as in the case when Q_a, Q_s^{tr} are directly proportional to the particle radius. In the last case, the corresponding coefficients don't depend on particle size distribution [12].

One should remember that physical approach discussed above is applicable only for weakly absorbing host med-

ium. The optical thickness of the medium at distances comparable with the particle size must be small: $\tau_0 = \alpha_0 a \ll 1$. In the opposite case, one cannot consider far-field characteristics of single particles and the traditional radiation transfer theory is inapplicable [14]. It is a limiting case of opaque medium when the volume radiative properties don't determine the reflection of radiation from the composite material. The details of mathematics concerning the efficiency factors calculation can be found elsewhere [2,12,15].

6. Comparison of theoretical predictions with experimental data

We consider the most interesting spectral ranges where the polymer is semi-transparent and considerable values of both reflectance and transmittance and observed in the experiments: $\lambda = 4.5$ μm and $\lambda = 11.5$ μm. The first of these ranges is characterized by the strongest peak of reflectance and it is a good chance to verify the theoretical model in the near infrared. The peak of reflectance at $\lambda = 11.5$ μm is not so strong but this spectral range is important for the problem of night cooling of buildings because of the transparency of clear sky in the range $8.5 < \lambda < 13.5$ μm [16–18].

The results of calculations are presented in Figs. 7 and 8. Two different assumptions were used for the microsphere wall thickness: the wall thickness was assumed constant or directly proportional to the radius of microsphere. The calculations were performed for two variants of glass optical constants corresponding to soda lime silica glass and low expansion borosilicate glass. The scattering is characterized by the transport efficiency factor Q_s^{tr} (Fig. 7) and absorption – by the absorption parameter $\alpha_1 = -Q_a/(4\alpha_0/3)$ (Fig. 8). The physical sense of the last parameter is clear from the expression for the absorption coefficient of composite material [4,8]:

$$\alpha = (1 - \alpha_1 f_v)\alpha_0 \tag{16}$$

One can see in Fig. 7 that variation of Q_s^{tr} with particle radius is not strong in the range of $a > 20$ μm both for constant and variable δ and the value of Q_s^{tr} is not sensitive to the type of microspheres. The difference between two variants of glass optical constants is small at the wavelength $\lambda = 4.5$ μm and significant at $\lambda = 11.5$ μm. In the first spectral range, one can use the value $Q_s^{tr} = 0.45$ for microspheres of radius a_{32}, whereas at wavelength 11.5 μm the following average values should be used: $Q_s^{tr} = 0.25$ for soda lime silica glass and $Q_s^{tr} = 0.1$ for borosilicate glass.

In contrast to the case of large bubbles in a weakly absorbing medium [4,8], the absorption parameter α_1 for hollow glass microspheres is not equal to unity even in the range $\lambda = 4.5$ μm (Fig. 8a) and $\alpha_1 < 0$ at the wavelength 11.5 μm (Fig. 8b). The negative values of α_1 show that absorption coefficient increases when glass microspheres are present in the polymer. In subsequent calculations,

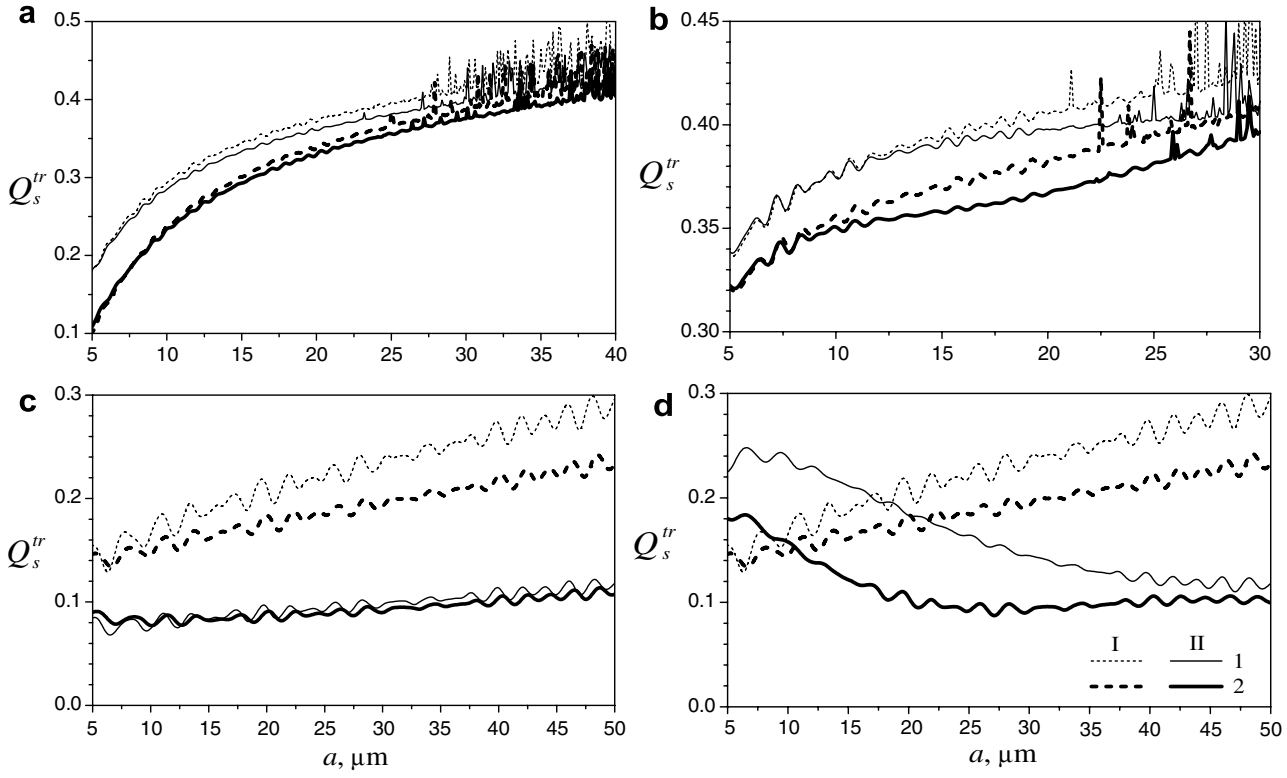

Fig. 7. Transport efficiency factor of scattering for single microspheres at $\lambda = 4.5$ μm (a and b) and $\lambda = 11.5$ μm (c and d) in the cases of $\delta = \bar{\delta}$ (a and c) and $\delta = \bar{\delta}a/a_{32}$ (b and d): (1) $\bar{\delta} = 1.3$ μm (K20), (2) $\bar{\delta} = 2.1$ μm (S38); (I) soda lime silica glass, (II) borosilicate glass.

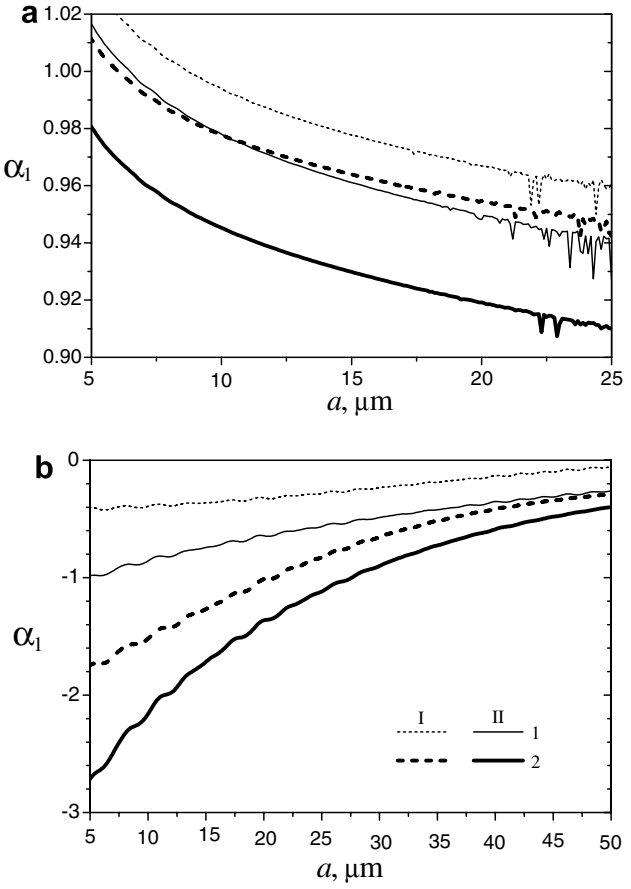

Fig. 8. Absorption parameter for single microspheres at the wavelength $\lambda = 4.5$ μm (a) and $\lambda = 11.5$ μm (b): (1) $\bar{\delta} = 1.3$ μm (K20), $\bar{\delta} = 2.1$ μm (S38); (I) soda lime silica glass, (II) borosilicate glass.

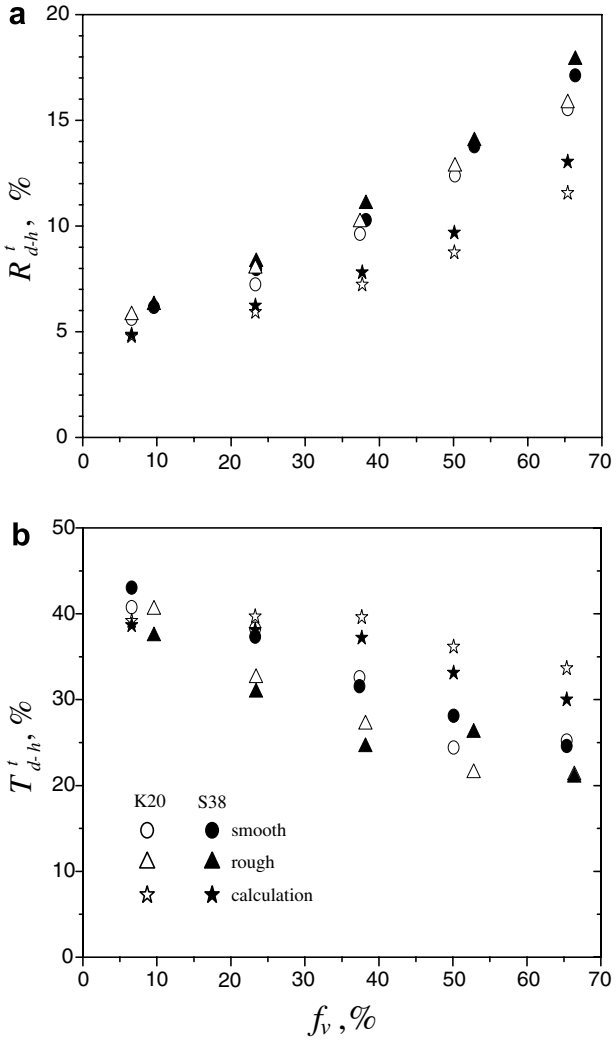

Fig. 9. Total direction-hemispherical reflectance (a) and transmittance (b) at the wavelength $\lambda = 4.5$ μm. Comparison of calculations experimental data for different orientations of the samples (smooth or rough front surface).

we use the average value $\alpha_1 = 0.9$ at $\lambda = 4.5$ μm and the following values at $\lambda = 11.5$ μm: $\alpha_1 = 0$ (K20), $\alpha_1 = -0.4$ (S38) for soda lime silica glass and $\alpha_1 = -0.3$ (K20), $\alpha_1 = -0.6$ (S38) for borosilicate glass.

The results of calculations of total directional-hemispherical reflectance and transmittance by use of modified two-flux approximation are presented in Figs. 9 and 10. The calculations were performed for the average values of sample thickness d and volume fraction of microspheres f_v from Table 1.

The systematic underestimation of the reflectance in the calculations at the wavelength 4.5 μm (Fig. 9a) can be partially explained by small additional reflection of radiation from the rough surface of the samples. Additional calculations showed that another possible reason of low predicted reflectance is the total internal reflection taken into account in the modified two-flux approximation. One can expect that effect of total internal refection decreases with the volume fraction of microspheres. The experimental data for directional-hemispherical reflectance do not show any specific behavior at high volume fraction of the microspheres. It means that dependent scattering has no significant effect on the reflectance. Note that this result was not evident. One can remember the recent study of microsphere ceramics [19]. At the same wavelength, the calculations of total directional-hemispherical transmittance give the results which are closer to the measurements of samples with smooth front surface (Fig. 9b). The difference between the results for microspheres of series K20 and S38 is approximately the same in the calculations and in the experiment. The role of optical properties of glass is negligible in this range. The theoretical model gives rather good qualitative description of the peaks of reflectance and transmittance at $\lambda = 4.5$ μm and their dependences on volume fraction and average size of microspheres.

At the wavelength 11.5 μm, the discrepancy between calculated and measured reflectance is significant (Fig. 10a). Comparison of the experimental results for different orientations of the samples shows that relatively large measured values of reflectance are explained by the roughness of front surface of the sample. The effect of roughness on reflectance is greater than the difference between two types

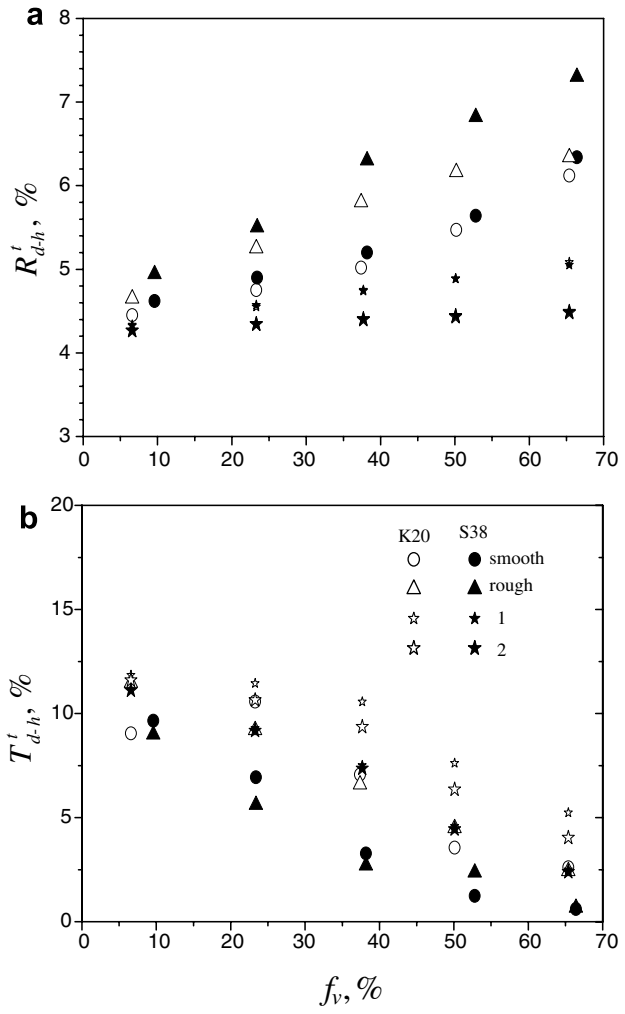

Fig. 10. Total direction-hemispherical reflectance (a) and transmittance (b) at the wavelength $\lambda = 11.5$ μm. Comparison of calculations ((1) soda lime silica glass, (2) borosilicate glass) with experimental data for different orientations of the samples (smooth or rough front surface).

of microspheres but the roughness is not taken into account in approximate radiation transfer model. The low transmittance at $\lambda = 11.5$ μm (Fig. 10b) is explained by absorption of radiation in the polymer and additional absorption in glass of microspheres. These effects are well described by theoretical model which shows that more than 90% of radiation is absorbed in the samples with high volume fraction of microspheres. Both measurements and calculations show that transmittance is considerably less in the case of thick-wall particles.

It should be noted that theoretical model cannot give good predictions of reflectance at the wavelength 11.5 μm because of too high absorption of the polymer. The above mentioned condition $\tau_0 \ll 1$ is not satisfied for particles of average radius a_{32}: $\tau_0 = 0.65$ for K20 and $\tau_0 = 0.53$ for S38 microspheres.

The experimental results showed small reflectance from the optically thick layer of the composite material in the spectral range $8.5 < \lambda < 13.5$ μm which is important for

Table 3
Directional integral emissivity of the polymer samples containing microspheres

Type of microspheres	Sample number	$\varepsilon(\theta)$				
		$\theta = 0$	20°	40°	50°	60°
K20	1	0.96	0.96	0.94	0.92	0.86
	5	0.89	0.89	0.88	0.87	0.77
S38	1	0.97	0.97	0.96	0.93	0.87
	5	0.92	0.92	0.92	0.90	0.82

radiative heat losses from the buildings. It means that decrease in integral hemispherical emissivity ε^h of the polymer coating due to presence of hollow glass microspheres is not expected to be significant. The integral emissivity of optically thick polymer samples in the wavelength range from 8 to 14 μm was measured directly by pyrometer CYCLOPS COMPAC 3S for several directions from $\theta = 0°$ to 60°. The samples were placed in a heated metal frame which is maintained at the temperature 373 ± 2 K. The measured values of $\varepsilon(\theta)$ with uncertainty ± 0.02 are given in Table 3. The high values of emissivity are in good agreement with the low reflectance of the samples in the range $8 < \lambda < 14$ μm (see Fig. 6).

7. The minimal emissivity of a polymer coating containing hollow microspheres

As was shown in the previous section, the decrease in the long-wave emissivity of polymer ACRONAL 290D by introducing the glass microspheres K20 and S38 produced by 3M Company is insignificant (about 10%) and explained mainly by surface effect at high volume fraction of microspheres in the polymer layer. It is interesting to analyze another possibility of a more considerable effect of hollow microspheres. The latter might be realized for not so absorbing coating when volume scattering is important. The comparison with experimental data showed that our theoretical model is applicable in this case.

Consider spectral hemispherical emissivity ε^h_λ of optically thick layer of a weakly absorbing coating. At large volume fraction of microspheres, the angular distribution of thermal radiation in the coating is expected to be smooth, without effect of total internal reflection. Following the paper [2], one can use the ordinary two-flux approximation which gives the following equation:

$$\varepsilon^h_\lambda = \frac{2\sqrt{1-\omega_{tr}}}{1+\sqrt{1-\omega_{tr}}/\gamma} \tag{17}$$

Note that the effect of the refractive index of polymer is likewise minor (at $n_0 = 1.5$, we have $\gamma = 0.92$ instead of $\gamma = 1$ at $n_0 = 1$). The transport albedo of the medium turns out to be the main parameter of the problem. A low emissivity of the coating can be obtained only in the case of a significant share of scattering in the extinction of radiation by the disperse system. The effect of surface roughness is ignored in Eq. (17). The previous analysis showed that it is a

reasonable assumption for the thermal radiation of a semi-transparent material in contrast to the case of strongly absorbing coating. In the case of a weakly absorbing medium ($\tau_0 \ll 1$), Eq. (17) can be simplified:

$$\varepsilon_\lambda^{\mathrm{h}} = 2\sqrt{p_\lambda}, \quad p_\lambda = \frac{\alpha}{\sigma_{\mathrm{tr}}} = \frac{4}{3}\frac{1-\alpha_1 f_{\mathrm{v}}}{f_{\mathrm{v}} Q_{\mathrm{s}}^{\mathrm{tr}}}\tau_0 \tag{18}$$

The calculations showed that parameter p_λ strongly depends on the wall thickness of glass microspheres in the range $8.5 < \lambda < 13.5$ μm and the best results can be obtained for microspheres with very thin walls [2] or for microspheres produced from a weakly absorbing material. In this limiting case, one can use the values $\alpha_1 = 1$ and $Q_{\mathrm{s}}^{\mathrm{tr}} = 0.9(n_0 - 1)$ for large gas bubbles in the polymer. The volume fraction of microspheres in the coatings is usually about 0.5–0.6. It corresponds approximately to the densely-packed microspheres. The index of refraction for the majority of polymers is 1.3–1.5. The resulting approximate relations are as follows:

$$p_\lambda \approx 3\tau_0, \quad \varepsilon_\lambda^{\mathrm{h}} = 3.5\sqrt{\tau_0} \tag{19}$$

It is clear that desirable value of emissivity about $\varepsilon_\lambda^{\mathrm{h}} = 0.35$ can be reached only in the case of $\tau_0 \approx 0.01$. For the average radius of particles $a_{32} = 50$ μm, we have the following estimate for the favourable absorption index of the polymer matrix: $\kappa \approx 2 \times 10^{-4}$.

The analysis showed that one should use thin-wall microspheres and a polymer with low absorption coefficient in wavelength range from 8.5 to 13.5 μm to reach the maximum decrease in integral emissivity of the coating.

8. Conclusions

The experimental investigation of infrared radiative characteristics of polymer films containing hollow glass microspheres has been performed. The spectral measurements of both total and diffuse components of the directional-hemispherical reflectance and transmittance in the range of $2.6 \leqslant \lambda \leqslant 18$ μm for near to the normal incidence of collimated radiation are performed for several samples containing different series of microspheres of volume fraction from about 6% to 66%. The effect of the roughness of the sample surface is also studied in the experiments.

The strong peak of reflectance is observed at the wavelength 4.5 μm. Position of the peak is the same for polydisperse glass microspheres of two different series. The maximum value of the total directional-hemispherical reflectance is not sensitive to the sample orientation (smooth or rough front surface of the sample). It enables us to analyze these results by use of the Fresnel boundary conditions at both sample surfaces. The calculations of total reflectance and transmittance on the basis of the modified two-flux approximation for radiative transfer in refracting and scattering medium and the Mie theory for hollow glass microspheres give the results which are in good qualitative agreement with the experimental data. It confirms an applicability of traditional radiation transfer theory and independent scattering approach even for the case of high volume fraction of microspheres in the polymer.

The reflectance of the polymer layer containing microspheres is of another nature in the important spectral range from 8.5 to 13.5 μm. In this range, the reflectance is determined mainly by rough surface layer of microspheres and is not described by the model suggested for a semi-transparent medium because of strong absorption in the polymer.

The analysis of spectral hemispherical emissivity of polymer coatings containing hollow glass microspheres showed that the most significant decrease in the emissivity in the spectral range from 8.5 to 13.5 μm and hence in radiative heat losses from the buildings can be expected for thin-wall microspheres and a polymer with low absorption in the above mentioned spectral range.

Acknowledgements

The authors are grateful to the 3M Company for the samples of glass microspheres and Verre Labo Mula Company for the samples of borosilicate glass.

Leonid Dombrovsky is also grateful to the Centre Thermique de Lyon (CETHIL) and the Russian Foundation for Basic Research (Grant No. 04-02-16014) for their partial financial support of the work.

References

[1] M.L. German, P.S. Grinchuk, Mathematical model for calculating the heat-protection properties of the composite coating "ceramic microspheres – binder", J. Eng. Phys. Thermophys. 75 (6) (2002) 1301–1313.

[2] L.A. Dombrovsky, Modeling of thermal radiation of a polymer coating containing hollow microspheres, High Temp. 43 (2) (2005) 247–258.

[3] A.P. Ivanov, V.A. Loiko, V.P. Dick, Propagation of Light in Densely Packed Dispersive Media, Nauka i Technika, Minsk, 1988 (Chapter 2, in Russian).

[4] S. Kumar, C.L. Tien, Dependent absorption and extinction of radiation by small particles, ASME J. Heat Transfer 112 (1990) 178–185.

[5] B.P. Singh, M. Kaviany, Modelling radiative heat transfer in packed beds, Int. J. Heat Mass Transfer 35 (6) (1992) 1397–1405.

[6] D. Baillis, J.-F. Sacadura, Thermal radiation properties of dispersed media: theoretical prediction and experimental characterization, J. Quant. Spectrosc. Radiat. Transfer 67 (5) (2000) 327–363.

[7] C. Coquard, D. Baillis, Radiative characteristics of opaque spherical particles beds: a new method of prediction, AIAA J. Thermophys. Heat Transfer 18 (2) (2004) 178–186.

[8] L. Dombrovsky, J. Randrianalisoa, D. Baillis, L. Pilon, Use of Mie theory to analyze experimental data to identify infrared properties of fused quartz containing bubbles, Appl. Opt. 44 (33) (2005) 7021–7031.

[9] M.F. Modest, Radiative Heat Transfer, second ed., Academic Press, New York, 2003 (Chapter 2).

[10] M. Rubin, Optical properties of soda lime silica glasses, Sol. Energy Mater. 12 (4) (1985) 275–288.

[11] L. Dombrovsky, J. Randrianalisoa, D. Baillis, Modified two-flux approximation for identification of radiative properties of absorbing and scattering media from directional-hemispherical measurements, J. Opt. Soc. Am. A 23 (1) (2006) 91–98.

[12] L.A. Dombrovsky, Radiation Heat Transfer in Disperse Systems, Begell House, New York, 1996 (Chapter 2).
[13] L.A. Dombrovsky, The propagation of infrared radiation in a semitransparent liquid containing gas bubbles, High Temp. 42 (1) (2004) 133–139.
[14] M.I. Mishchenko, J.W. Hovenier, D.W. Mackowski, Single scattering by a small volume element, J. Opt. Soc. Am. A 21 (1) (2004) 71–87.
[15] C.F. Bohren, D.R. Huffman, Absorption and Scattering of Light by Small Particles, Wiley, New York, 1983 (Chapters 4 and 7).
[16] P. Berdahl, R. Fromberg, The thermal radiance of clear skies, Sol. Energy 29 (4) (1982) 299–314.
[17] A. Skartveit, J.A. Olseth, G. Czeplak, M. Rommel, On the estimation of atmospheric radiation from surface meteorological data, Sol. Energy 56 (4) (1996) 349–359.
[18] X. Berger, J. Bathiebo, Directional spectral emissivities of clear skies, Renew. Energy 28 (12) (2003) 1925–1933.
[19] L.A. Dombrovsky, Approximate models of radiation scattering in hollow-microsphere ceramics, High Temp. 42 (5) (2004) 772–779.